Prachi., 2026, 14:4
ISSN (Online): 2348-4098
ISSN (Print): 2395-4752

International Journal of Science, Engineering and Technology
An Open Access Journal

Identification and Performance Evaluation of Metamaterial Geometries and Integration Configurations for Multiband Microstrip Patch Antenna Applications

Prachi[1], Sharad Kumar[2]
[1]Research Scholar, Department of Electronics & Communication Engineering, Shri Venkateshwara University, Gajraula India,
[2]Associate Professor, Department of Electronics & Communication Engineering, Shri Venkateshwara University,

Abstract- Metamaterial-inspired loading offers additional degrees of freedom for developing compact multiband microstrip antennas, but performance depends on how resonators interact with the complete radiating structure. This paper identifies representative resonator geometries and integration configurations through a focused narrative examination of foundational electromagnetic studies and selected antenna demonstrations. Split-ring, complementary split-ring, electric-LC, and patterned-surface approaches are compared according to excitation mechanism, modal control, fabrication demands, and radiation implications. Published examples are distinguished from the analytical framework proposed here; no new electromagnetic simulation or experimental measurements are claimed. The synthesis indicates that planar complementary resonators provide practical candidates for introducing additional resonances, whereas elevated metamaterial structures address directivity through a different spatial mechanism. Neither approach establishes universal superiority because substrate properties, electrical dimensions, ground configuration, and measurement conventions vary across studies. A controlled evaluation protocol is developed using bandwise impedance bandwidth, realized gain, radiation efficiency, normalized size, current distributions, and tolerance sensitivity. The central conclusion is that geometry and integration must be selected jointly, with usable radiation performance and reproducibility taking precedence over resonance count or exceptionally deep reflection minima.

Keywords— metamaterial-inspired antenna, microstrip patch, split-ring resonator, multiband operation, integration configuration, performance evaluation

I. INTRODUCTION

A multiband antenna must provide useful radiation over several specified frequency intervals within a practical mechanical envelope. The design problem therefore extends beyond producing multiple minima in a reflection-coefficient plot. A compact radiator may match well while dissipating substantial power, radiating toward an unsuitable direction, or failing to cover the required channel edges. For microstrip patch applications, any additional resonant structure must be assessed together with its feed, substrate, finite ground plane, and installation environment.

Metamaterial research established that conducting inclusions can generate electromagnetic responses unavailable from their constituent bulk materials alone. Pendry et al. (1999) demonstrated the basis for artificial magnetic response using structured conductors. This insight motivates antenna loading, but it does not imply that every patterned slot constitutes a homogeneous negative-index material. In finite antennas, a small number of resonators can instead function as localized reactive elements. Distinguishing these interpretations is necessary before attributing an observed improvement to a particular physical mechanism.

The title of this study addresses two linked questions: which geometries are useful candidates, and where should they be integrated? Published designs demonstrate that several structural interventions can contribute to the final response. For example, Malik and Kartikeyan (2012) combined complementary resonator loading with a modified ground, while Mahdy et al. (2011) combined material loading, slots, and parasitic adjustment. These examples motivate a comparison based on mechanisms and controls rather than decorative similarity between layouts.

This paper contributes a geometry–integration taxonomy, a bounded comparison of published evidence, and a reproducible evaluation framework. Its scope is primarily passive microwave patch structures, with one recent printed-monopole example included explicitly as adjacent evidence. The intended outcome is a defensible selection procedure for subsequent numerical and experimental work, rather than an unsupported ranking of resonator shapes.

II. REVIEW METHOD AND EVIDENCE BOUNDARIES

A focused narrative search was conducted on 7 September 2026 using combinations of "multiband microstrip patch antenna," "split-ring resonator," "complementary split-ring resonator," "metamaterial loading," and "gain enhancement." Publisher pages, article abstracts, accessible full texts, and author-hosted materials were consulted. Foundational sources were retained for physical interpretation, while antenna demonstrations were selected for their relevance to distinct integration mechanisms. The resulting ten-reference set is purposive and is not presented as an exhaustive systematic review.

Inclusion required identifiable bibliographic information and a clear connection to resonator physics, parameter extraction, patch integration, or antenna evaluation. Broad reviews and unverified secondary summaries were not used as numerical evidence. Reported quantities were retained with their original meaning: a gain increase in decibels was not converted into an absolute gain in dBi, and directivity was not relabeled as realized gain. Where accessible reporting did not support a numerical comparison, the study was discussed qualitatively.

Three evidence categories organize the analysis. Foundational investigations explain electromagnetic mechanisms. Selected antenna studies establish that particular combinations can work under their reported conditions. The proposed protocol specifies how a future controlled comparison should be performed. Statements about recommended controls, acceptance rules, and reporting templates are methodological proposals of this paper, not results obtained from fabricated prototypes.

Cross-study pooling was avoided because the selected structures differ in topology, substrate, operating frequency, aperture, and validation detail. Consequently, this paper neither estimates an average performance improvement nor assigns statistically supported superiority to one geometry. Table 1 provides the classification used throughout the discussion, while Table 2 records a small set of source-specific observations.

III. ELECTROMAGNETIC BASIS AND GEOMETRY IDENTIFICATION

1. Resonant loading and its interpretation

A first-order resonator model represents the dominant inductive and capacitive storage using an approximate resonance frequency:

$$f_0 \approx 1 / (2\pi\sqrt{(LC)}) \qquad (1)$$

Here, L and C are effective quantities for the selected mode, rather than universal constants attached to a shape. Equation (1) explains why increasing the current path or capacitive interaction can lower a resonance. It cannot predict the complete antenna response without coupling, losses, and radiation. Multiple resonators may produce hybrid modes, so the number of visible operating bands need not equal the number of inclusions.

The magnetic response of split-ring arrangements depends on excitation and orientation (Pendry et al., 1999). Complementary split-ring resonators were introduced in a microstrip stopband configuration by Falcone et al. (2004), where etched ground features produced resonant rejection. That result is particularly instructive: a useful filter resonance is not automatically a useful radiating band. Antenna integration must demonstrate that accepted energy produces the intended far field.

Schurig et al. (2006) developed electric-field-coupled resonators with a strong electric response, providing a distinct route from magnetic-loop loading. These resonators offer a means of selecting electric coupling through their capacitive region. For antenna screening, this suggests comparing candidate locations using the unmodified structure's local field orientation, rather than assuming that the patch center is always the preferred location.

Table 1: Geometry Families and Primary Screening Considerations

Family	Primary interaction	Key screening issue
SRR	Loop and gap resonance	Field orientation; conductor loss
CSRR / OCSRR	Complementary slot resonance	Slot coupling; current disruption
Electric-LC	Electric-field coupling	Capacitive-gap alignment
Patterned surface	Surface boundary response	Finite extent; operating band

Note. SRR = split-ring resonator; CSRR = complementary SRR; OCSRR = open CSRR. Classification synthesized from Pendry et al. (1999), Falcone et al. (2004), Schurig et al. (2006), and Sievenpiper et al. (1999).

2. Effective-medium claims and finite structures

Smith et al. (2002) established retrieval of effective permittivity and permeability from reflection and transmission coefficients. Such extraction can support material characterization, but it requires a defined excitation, sample thickness, and interpretation of the retrieved branches. Parameters obtained from a periodically repeated unit cell should not be treated as a complete explanation of a single inclusion near an antenna feed.

The proposed reporting convention is therefore conservative. A finite loaded antenna may be described as metamaterial-inspired when its response is explained through resonant inclusions. Stronger claims of negative-index behavior should include appropriate constitutive evidence and establish relevance to the operating field configuration. Current maps, modal behavior, and controlled removal of inclusions should accompany any retrieval plot.

High-impedance surfaces introduce another mechanism. Sievenpiper et al. (1999) investigated patterned electromagnetic surfaces with forbidden propagation bands. These surfaces should be characterized through their surface response and propagation behavior, rather than presumed equivalent to a bulk double-negative slab. Their inclusion in the taxonomy reflects their relevance to boundary engineering; it does not make every electromagnetic-bandgap structure interchangeable with a split-ring medium.

IV. INTEGRATION CONFIGURATIONS AND MODAL CONTROL

Patch-etched loading places a complementary resonator directly within the radiator. Its principal design advantage is access to the patch's local electric field without necessarily adding another board layer. Its central risk is disruption of an existing radiating mode. A candidate that introduces the desired lower band may also shift the upper band, increase cross-polarization, or concentrate current in narrow bridges. The recommended control is a same-footprint patch with an ordinary slot of comparable occupied area.

Ground-plane loading modifies return-current paths and coupling through the substrate. It can offer another degree of freedom when patch area is constrained, but the full ground boundary remains part of the antenna. A shortened or heavily slotted ground can change the radiator's classification and radiation behavior. Figure 1 separates these positions from substrate and superstrate loading so that a comparison does not silently combine different physical architectures.

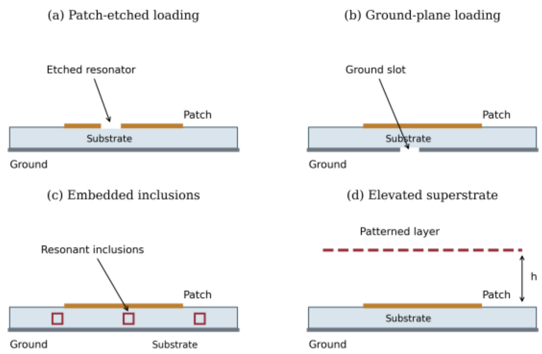

Figure 1: Representative Integration Positions in a Patch Antenna Assembly

Note. Original conceptual cross-sections; not to scale and not fabrication drawings. Dashed marks indicate the patterned superstrate; h denotes separation. Integration categories illustrate the mechanisms discussed in Sections 3–4.

Embedded inclusions offer access to fields beneath the patch, but introduce layer alignment and material-characterization demands. Nearby parasitic resonators offer adjustable coupling through separation and orientation. Both should be screened for dependence on manufacturing tolerances and nearby conductors. For a controlled study, their total occupied volume must include clearances and supporting layers, not only the metallic patch dimensions.

A superstrate places a patterned structure above the radiator and can reshape the emitted field. Majid et al. (2009) reported a gain increase of up to 4 dB and an impedance-bandwidth change from 2.9% to 4.98% for their loaded patch arrangement. This is evidence for that particular assembly, not proof that an elevated layer will improve every band of a multiband antenna. Its height and lateral extent must be included in any compactness comparison.

Hybrid integration combines two or more interventions. The additional variables can help separate band control, but they also make causal explanation harder. Accordingly, this paper proposes adding one intervention at a time and recording which resonance shifts, appears, or disappears. Feed retuning should be documented separately because improved matching may otherwise be attributed entirely to the added metamaterial geometry.

V. COMPARATIVE FINDINGS FROM PUBLISHED STUDIES

Table 2 summarizes selected demonstrations without presenting them as a common benchmark. Malik and Kartikeyan (2012) associated the upper 5.8 GHz band with CSRR loading and the lower 3.5 GHz band with an L-shaped ground slot. Their design included prototype measurements. The useful lesson is the allocation of distinct structural roles, rather than a general claim that CSRRs necessarily produce the upper band in every antenna.

Mahdy et al. (2011) reported a triple-band rectangular patch concept involving a modified mode, symmetric slots, and parasitic adjustment. This example supports investigation of hybrid modal control. However, its numerical performance is not pooled with measured results here because the present comparison does not reconstruct equivalent validation conditions across studies.

Christydass et al. (2025) reported an OCSRR-loaded, offset-fed rectangular printed monopole with resonances at 3.16, 3.82, and 5.41 GHz on a 27.84 × 23.25 × 1.6 mm substrate. Its reduced-ground topology makes it adjacent evidence rather than a direct full-ground patch benchmark. The example shows why terminology and geometry must be checked before compiling comparison tables.

Table 2: Selected Published Demonstrations and Limits of Comparison

Study	Configuration and observation	Evidence boundary
Malik & Kartikeyan (2012)	Patch CSRR + ground slot; 3.5 and 5.8 GHz	Simulation and prototype measurements
Mahdy et al. (2011)	Loaded rectangular patch; three-band modal design	Qualitative design evidence here

Study	Configuration and observation	Evidence boundary
Majid et al. (2009)	External SRR/CLS structure; gain increase up to 4 dB	Single-patch enhancement; not multiband proof
Christydass et al. (2025)	OCSRR + offset feed; 3.16, 3.82, 5.41 GHz	Measured/simulated monopole study

Note. Observations are attributed to the listed publications and are not new results. CLS = capacitance-loaded strip. Different antenna types and conditions prevent direct ranking.

Together, these observations support three bounded findings. First, multiple operating bands may result from cooperation between resonators and conventional features. Second, radiation enhancement using an external layer answers a different question from resonance creation within a planar radiator. Third, published performance cannot be transferred between geometries without controlling the reference antenna and installation conditions.

These findings also expose a common comparison error: selecting the deepest reflection minimum as the best antenna. Reflection establishes only the mismatch contribution to accepted power. A lossy inclusion can change the input impedance without delivering a corresponding radiation benefit. Therefore, the evaluation proposed below treats impedance, efficiency, radiation pattern, and size as separate outcomes before considering an overall preference.

VI. PROPOSED PERFORMANCE EVALUATION FRAMEWORK

1. Common baseline and candidate matrix

A future comparison should begin with declared operating intervals, required polarization, coverage direction, maximum enclosure dimensions, and a feasible fabrication process. The unloaded baseline should use the same substrate family, conductor model, feed reference plane, and connector arrangement as the candidates. Geometry comparisons should then distinguish fixed-footprint experiments from equal-frequency miniaturization experiments; these answer different questions.

The initial candidate matrix should contain an unloaded reference, patch-loaded resonator, ground-loaded resonator, parasitic resonator, and optional superstrate. Each should first be evaluated with a controlled feed and then with a separately optimized feed. This two-stage arrangement distinguishes the consequences of loading from the benefits of impedance retuning. A non-metamaterial slot or parasitic control should be included wherever a simpler feature could plausibly produce the same additional resonance.

2. Bandwise metrics and normalization

For each connected matched interval, fractional impedance bandwidth should be computed as:

$$FBW = 100(f_H - f_L) / [(f_H + f_L)/2] \quad (2)$$

The frequencies f_L and f_H are the lower and upper threshold crossings for that interval. This protocol adopts $S_{11} \leq -10$ dB as its declared comparison threshold; an application may require another value. Separate intervals should never be merged across an unmatched gap. Both band edges and the selected center-frequency definition should be reported to make Equation (2) reproducible.

Normalized dimensions should use the same reference wavelength, preferably the free-space wavelength at the lowest required operating frequency. Total board length, width, and assembly height should be retained alongside normalized values. Area reduction should be calculated only against a baseline providing comparable frequency coverage and radiation requirements. A smaller patch on a larger support board is not necessarily a smaller antenna assembly.

For a single-port antenna, using linear quantities and a common reference plane, realized gain can be expressed as:

$$G_r(\theta, \varphi) = D(\theta, \varphi)\, \eta_{rad}\, (1 - |\Gamma|^2) \quad (3)$$

Here, D is directivity, ηrad is radiation efficiency, and Γ is the input reflection coefficient. Equation (3) makes the measurement distinction explicit. In this framework, radiation efficiency excludes mismatch, while total efficiency includes it. Reporting should state whether cable and connector losses have been removed. Table 3 defines the minimum comparison record.

Table 3: Minimum Record for a Controlled Performance Comparison

Metric	Required reporting	Purpose
Impedance bandwidth	Threshold; fL; fH; FBW per band	Verify complete coverage
Realized gain	Bandwise values; direction; dBi	Include mismatch effects
Efficiency	Radiation and total efficiency	Separate dissipation from mismatch
Radiation pattern	Co-/cross-polarization; band edges	Verify coverage and polarization
Electrical size	Full L × W × H; common λ_0	Compare complete assemblies
Robustness	Tolerances; cases; pass fraction	Assess repeatability

Note. Proposed reporting framework developed in this paper; these entries are requirements, not measured performance.

3. Simulation, measurement, and attribution

Full-wave simulation should include finite ground dimensions, dielectric and conductor losses, and the relevant feed transition. Mesh refinement must target narrow gaps and slot edges, with convergence checked for resonance position and radiation metrics. A small movement in a deep S_{11} minimum is insufficient evidence of convergence if efficiency or peak direction remains unstable.

The mechanism study should plot surface currents and relevant near fields at each band. Removing one inclusion, rotating it, or changing its coupling gap provides a practical attribution test. A resonance that persists with little change after removing the supposed active feature should not be assigned to that feature without another explanation. Equivalent circuits may support interpretation, but fitted circuit agreement alone does not validate the proposed radiation mechanism.

Experimental validation should combine calibrated input measurements with gain, efficiency, and pattern characterization over each operating interval. Measurements at the band edges are needed because center-frequency performance can conceal coverage failure. Prototype photographs, fabrication dimensions, substrate identification, calibration plane, and chamber arrangement should be reported. Repeated samples are preferable when narrow slots or strong coupling make the design sensitive to fabrication variation.

4. Robustness and selection rules

This paper proposes tolerance sweeps for etching gap, conductor width, substrate thickness, permittivity, and layer registration using actual fabrication specifications. The outcome should be expressed as the fraction of evaluated cases satisfying all declared bands and radiation requirements. Such a yield estimate requires documented distributions or bounded assumptions; it must not be presented as a measured production yield unless production data exist.

Selection should begin with mandatory feasibility checks. Designs that fail a required band, efficiency floor, or mechanical limit are rejected before ranking. Among feasible candidates, Pareto comparison can expose trade-offs between size, minimum bandwise realized gain, bandwidth margin, and fabrication complexity. If a weighted score is used, its weights must come from the intended application, with sensitivity analysis showing whether the preferred geometry changes under reasonable alternatives.

VII. DISCUSSION, LIMITATIONS, AND RESEARCH DIRECTIONS

The synthesis favors a staged decision process rather than a universal geometry recommendation. For a planar multiband objective, a complementary resonator is a reasonable candidate to investigate because it can be integrated into existing metallization. For an aperture or directivity objective with available height, an external patterned layer deserves separate evaluation. These are screening judgments derived from mechanisms, not validated rankings or promises of performance.

Miniaturization also requires physical restraint. Chu (1948) established fundamental connections between electrical size and radiation quality factor under idealized conditions. Metamaterial loading does not remove the need to account for stored energy and radiation. Claims of simultaneous large size reduction, broad bandwidth, and high efficiency deserve especially careful examination of assembly dimensions, losses, and measurement definitions.

The main limitation is the narrow, purposive evidence base. The study is not a comprehensive survey of every geometry or recent publication, and the selected sources cannot establish effect sizes or confidence intervals. No original S-parameters, radiation patterns, or fabrication data were generated. Consequently, the proposed evaluation protocol remains to be validated through a controlled campaign using common substrates, comparable frequency targets, and independent measurements.

Future research should publish reusable geometry files and raw bandwise measurements, compare metamaterial-inspired candidates against ordinary multiresonant controls, and include installation sensitivity. Optimization studies should retain designs that remain feasible after tolerance perturbation rather than reporting only a nominal optimum. Reporting unsuccessful candidates would also clarify which coupling choices fail and reduce repeated trial-and-error design.

VIII. CONCLUSION

Metamaterial geometries must be assessed together with their integration configurations. Split-ring, complementary, electric-LC, and patterned-surface structures offer different ways to influence local resonance or radiation boundaries. Selected studies demonstrate useful implementations, but heterogeneous conditions prevent a defensible universal ranking. The proposed framework requires a common baseline, controlled structural changes, bandwise bandwidth and radiation metrics, complete size normalization, and tolerance evaluation. Its practical contribution is a transparent path from geometry identification to experimentally defensible selection. A successful multiband antenna is one that meets its complete operating requirements reproducibly, rather than one that merely exhibits additional resonances.

Declarations
This manuscript is a literature-based analytical study. No new experimental dataset was generated. Numerical observations belong to the cited publications. Funding, competing-interest, authorship, and affiliation statements must be supplied and verified by the submitting authors. Similarity has not been measured; the manuscript requires an independent similarity check before submission.

REFERENCES

1. Christydass, S. P. J., Samithas, D., Balachandran, P. K., & Mohd Zainuri, M. A. A. (2025). Open complementary split-ring resonator-embedded tri-band rectangular monopole antenna with offset feed for next-gen wireless applications. Scientific Reports, 15, Article 35658. https://doi.org/10.1038/s41598-025-19455-z
2. Chu, L. J. (1948). Physical limitations of omni-directional antennas. Journal of Applied Physics, 19(12), 1163–1175. https://doi.org/10.1063/1.1715038
3. Falcone, F., Lopetegi, T., Baena, J. D., Marqués, R., Martín, F., & Sorolla, M. (2004). Effective negative-ε stopband microstrip lines based on complementary split ring resonators. IEEE

Microwave and Wireless Components Letters, 14(6), 280–282. https://doi.org/10.1109/LMWC.2004.828029

4. Mahdy, M. R. C., Zuboraj, M. R. A., Ovi, A. A. N., & Matin, M. A. (2011). Novel design of triple band rectangular patch antenna loaded with metamaterial. Progress In Electromagnetics Research Letters, 21, 99–107. https://doi.org/10.2528/PIERL10112005
5. Majid, H. A., Rahim, M. K. A., & Masri, T. (2009). Microstrip antenna's gain enhancement using left-handed metamaterial structure. Progress In Electromagnetics Research M, 8, 235–247. https://doi.org/10.2528/PIERM09071301
6. Malik, J., & Kartikeyan, M. V. (2012). Metamaterial inspired patch antenna with L-shape slot loaded ground plane for dual band (WiMAX/WLAN) applications. Progress In Electromagnetics Research Letters, 31, 35–43. https://doi.org/10.2528/PIERL12021908
7. Pendry, J. B., Holden, A. J., Robbins, D. J., & Stewart, W. J. (1999). Magnetism from conductors and enhanced nonlinear phenomena. IEEE Transactions on Microwave Theory and Techniques, 47(11), 2075–2084. https://doi.org/10.1109/22.798002
8. Schurig, D., Mock, J. J., & Smith, D. R. (2006). Electric-field-coupled resonators for negative permittivity metamaterials. Applied Physics Letters, 88(4), Article 041109. https://doi.org/10.1063/1.2166681
9. Sievenpiper, D., Zhang, L., Broas, R. F. J., Alexopolous, N. G., & Yablonovitch, E. (1999). High-impedance electromagnetic surfaces with a forbidden frequency band. IEEE Transactions on Microwave Theory and Techniques, 47(11), 2059–2074. https://doi.org/10.1109/22.798001
10. Smith, D. R., Schultz, S., Markoš, P., & Soukoulis, C. M. (2002). Determination of effective permittivity and permeability of metamaterials from reflection and transmission coefficients. Physical Review B, 65(19), Article 195104. https://doi.org/10.1103/PhysRevB.65.195104